AIP | Journal of Applied Physics

Negative resistance phenomenon in dual-frequency capacitively coupled plasma-enhanced chemical vapor deposition system for photovoltaic manufacturing process

H. C. Kwon, AmanurRehman, I. H. Won, W. T. Park, and J. K. Lee

Citation: J. Appl. Phys. **111**, 023305 (2012); doi: 10.1063/1.3679107
View online: http://dx.doi.org/10.1063/1.3679107
View Table of Contents: http://jap.aip.org/resource/1/JAPIAU/v111/i2
Published by the American Institute of Physics.

Negative resistance phenomenon in dual-frequency capacitively coupled plasma-enhanced chemical vapor deposition system for photovoltaic manufacturing process

H. C. Kwon,[1] Aman-ur-Rehman,[1,2] I. H. Won,[1] W. T. Park,[3] and J. K. Lee[1,a)]
[1]*Department of Electrical Engineering, Pohang University of Science and Technology, Pohang 790-784, South Korea*
[2]*Pakistan Institute of Engineering and Applied Sciences, P. O. Nilore, Islamabad 45650, Pakistan*
[3]*SEMES CO., LTD. #278 Mosi-ri, Jiksan-eup, Cheonan-si, Chungnam 331-814, South Korea*

(Received 26 August 2011; accepted 22 December 2011; published online 26 January 2012)

The validity of effective frequency concept is investigated for dual-frequency (DF) capacitively coupled plasma (CCP) discharges by using particle-in-cell/Monte Carlo collision simulations. This concept helps in analyzing DF CCP discharges in a fashion similar to single-frequency (SF) CCP discharges with effective parameters. Unlike the driving frequency of SF CCP discharges, the effective frequency in DF CCP is dependent on the ratio of the two driving currents (or voltages) and this characteristic makes it possible to control the ion flux and the ion bombardment energy independently. This separate control principally allows to increase the ion flux and plasma density for high deposition rates, while keeping the ion mean energy constant at low values to prevent the bombardment of highly energetic ions at the substrate surface to avoid unwanted damage in the solar cell manufacturing. The abrupt transition of the effective frequency leads to the phenomenon of negative resistance which is one of the several physical phenomena associated uniquely with DF CCP discharges. Using effective frequency concept, the plasma characteristics have been investigated in the negative resistance regime for solar cell manufacturing. © *2012 American Institute of Physics*. [doi:10.1063/1.3679107]

I. INTRODUCTION

Dual-frequency (DF) capacitively coupled plasma (CCP) discharges are being used to have a separate control over the ion mean energies and fluxes at the substrate.[1–10] This separate control of the mean energy and flux of the charged particles in capacitively coupled radio frequency discharges is one of the most important issues for various applications in plasma processing.[11,12] For instance, in the Plasma Enhanced Chemical Vapor Deposition (PECVD) processes which are used for solar cell manufacturing, this separate control is most relevant. By applying suitable combination of low and high frequency power sources, the DF CCP discharges can be used to increase the ion flux at the substrate for higher deposition rates, while the ion mean energy can be kept low to avoid damage caused by the bombardment of highly energetic ions at the substrate.[13–15] In view of low-cost manufacturing for plasma-synthesized silicon thin-film solar cells, high deposition rates without any compromise on cell efficiency are desirable. In conventional single frequency (SF) capacitively coupled radio frequency PECVD processes, however, high deposition rate for a device grade μc-Si:H or a-Si:H films are generally difficult due to problems such as coupling of ion bombardment energy and flux along with powder formation, which are encountered very often.[16,17] Bombardment of high-energy ions at the substrate surface often results in excessive defect formation, and hence significant deterioration of the film quality. The achievement of high growth rates without compromising quality of the deposited thin film is an important issue in the field of Si-based thin-film solar cell manufacturing.

DF CCP discharges can be analyzed in a fashion similar to SF CCP discharges by defining effective parameters.[5,18–20] It means that a DF CCP discharge can be treated as a SF CCP discharge with effective parameters such as effective frequency and effective current density. When one of the two power sources in a DF CCP discharge is much stronger than the other, then DF CCP discharge behaves as a SF CCP discharge operated with the stronger power source of the two and in this case one can say that the effective frequency simply corresponds to the driving frequency of the stronger power source in terms of the effective frequency concept. When the current (or voltage) of the other power source increases, the effective frequency moves from the frequency of the stronger power source to that of weaker power source. This is called transition of the effective frequency. The effective frequency in a DF CCP discharge is dependent on the ratio of the two driving currents (or voltages) unlike the fixed driving frequency in a SF CCP discharge. This characteristic of the DF CCP discharges may lead to a physical phenomenon called negative resistance.[18] The negative resistance means that the voltage decreases when current is increased. This physical phenomenon is induced due to abrupt transition of the effective frequency. As the high-frequency current increases, the square of the effective frequency increases more rapidly as compared to the effective current. As a result, the effective voltage decreases with the effective current and it leads to an increase in the ion flux for high deposition rates and a decrease of the ion mean energy to avoid

a)Author to whom correspondence should be addressed. Electronic mail: jkl@postech.ac.kr.

unwanted damage on the substrate surface. Because of that, the negative resistance regime can be called the preferred regime for solar cell manufacturing.

In this paper, we have investigated the validity of describing DF CCP discharges in terms of SF CCP discharges driven with effective parameters. Particle-in-cell/Monte Carlo Collision (PIC/MCC) simulations have been carried out to make comparison of plasma characteristics between DF CCP discharges and equivalent effective frequency operated SF CCP discharges under the same applied effective current conditions. We have also investigated the preferred regime (negative resistance regime) in DF CCP discharges for solar cell manufacturing by using effective frequency concept. The comparison of plasma characteristics between DF CCP and SF CCP under the same applied effective current condition is carried out in the negative resistance regime. The analytical model and the effective frequency concept are described in Sec. II. In this section, analytical expressions are obtained for discharge parameters such as the plasma density and the plasma potential. The negative resistance regime is explained in terms of the effective frequency concept. Section III shows the PIC-MCC simulation results for the validity of the effective frequency concept. The simulation results for the comparison of DF CCP and SF CCP discharges in the negative resistance regime are also shown in Sec. III. The summary is given in Sec. IV.

II. DESCRIPTION OF MODELS

The analytical expressions for a dual frequency capacitive discharge parameters are obtained as a function of effective frequency, effective current, and effective voltage by assuming time-independent collisionless ions motion. The electrons are assumed to be inertialess in these calculations. The details of the effective parameter concept for a dual frequency capacitive discharge are given in Refs. 5, 18, and 19. A brief description of the model is given below. Kim *et al.*[5] have shown that the plasma parameters of a DF CCP discharge can be expressed in terms of a SF CCP discharge, driven with effective parameters by using a homogeneous model. The effective parameters are given by

$$J_{eff} = J_p\sqrt{1+J_r^2}, \tag{1}$$

$$V_{eff} = V_p\left(1+V_r-\frac{2}{3}\frac{V_r}{1+V_r}\right), \tag{2}$$

and

$$f_{eff}^2(f_p,f_r,J_r) = f_p^2\frac{1+J_r^2}{1+4J_r/3f_r+J_r^2/f_r^2} \tag{3}$$

or

$$f_{eff}^2(f_p,f_r,V_r) = f_p^2\frac{1+(f_rV_r)^2}{(1+V_r)(1+V_r-\frac{2}{3}\frac{V_r}{1+V_r})}, \tag{4}$$

with $J_r = J_s/J_p$ and $V_r = V_s/V_p$. Here J_p and V_p are amplitudes of the rf current and rf voltage of the primary rf source, respectively, while J_s and V_s are amplitudes of the rf current and rf voltage of the secondary rf source, respectively. The effective frequency in DF CCP discharge is dependent on the currents or voltages of the two sources. In contrast to SF CCP discharges where the frequency is constant, the DF CCP discharges can be considered as SF CCP discharges with a variable effective frequency. Thus, the plasma density and time-averaged plasma potential can be expressed as a function of effective operating parameters (such as current density, voltage, and frequency). The plasma density is obtained by equating the total time-averaged electron power per unit area to the electron energy loss[5] and is given by

$$n = \frac{1}{2}\left[\frac{m(\nu_m d+2\bar{\nu}_e)}{e^3u_B(\varepsilon_c+\varepsilon_e)}\right]^{1/2}J_{eff}. \tag{5}$$

Substituting Eqs. (10) and (16) in Ref. 5, the time-averaged plasma potential can be expressed as a function of effective operating parameters (effective current density and frequency) and is given by

$$\overline{V} = \frac{3}{8}V_{eff} = \frac{3}{4en\varepsilon_0}\frac{J_{eff}}{\omega_{eff}^2} = \frac{3}{8\pi^2\varepsilon_0}\left[\frac{eu_B(\varepsilon_c+\varepsilon_e)}{m(\nu_m d+2\bar{\nu}_e)}\right]^{1/2}\frac{J_{eff}}{f_{eff}^2}. \tag{6}$$

Here, m, d, and $\bar{\nu}_e$ are the electron mass, the bulk plasma length, and the electron mean speed ($\bar{\nu}_e = \sqrt{8eT_e/m\pi}$, where T_e is the electron temperature), respectively. The bulk plasma length is given by the difference between the gap distance and the sheath length: $d = L - 2\bar{s}$. The terms ν_m, ε_c, and ε_e are the momentum transfer frequency for electron-neutral collision, collisional energy loss per electron-ion pair created, and mean kinetic energy lost per electron ($=2T_e$), respectively. The term u_B is the Bohm velocity ($u_B = \sqrt{eT_e/M}$). The values of T_e, ε_c, and L are taken to be 1.75 V, 200 V, and 1 cm, respectively, for making calculations. Figure 1 shows the effective voltages and the transition of effective frequency as a function of effective current obtained from Eqs. (1), (3), and (6) in dual frequency discharges when the high-frequency (40∼200 MHz) current is varied and the low-frequency (13.56 MHz) current is fixed ($J_l = 2$ mA cm^{-2}).

Since the effective frequency depends on the ratio of the two driving currents or voltages, physical phenomenon of negative resistance associated with DF CCP discharges cannot be observed in SF CCP discharges because of the presence of only one current or voltage. The phenomenon of negative resistance (the voltage decreases with increase in current) is induced due to abrupt transition of the effective frequency. As shown in Figure 1(a), the negative resistance is found in the regime of the small effective current, i.e., when the high frequency current changes and the low frequency (13.56 MHz) current ($J_l = 2$ mA cm^{-2}) is fixed. In SF CCP discharges, the rf voltage is proportional to the applied rf current and inversely proportional to the square of the frequency ($V_{rf} \propto J_{rf}/f^2$).[11] In DF CCP discharges, however, both the effective current and the effective frequency increase as the high-frequency current is increased. The negative resistance arises from the competition of the effective current and the effective frequency. As the high-frequency current increases, the square of the effective frequency increases more rapidly as compared to the effective current.

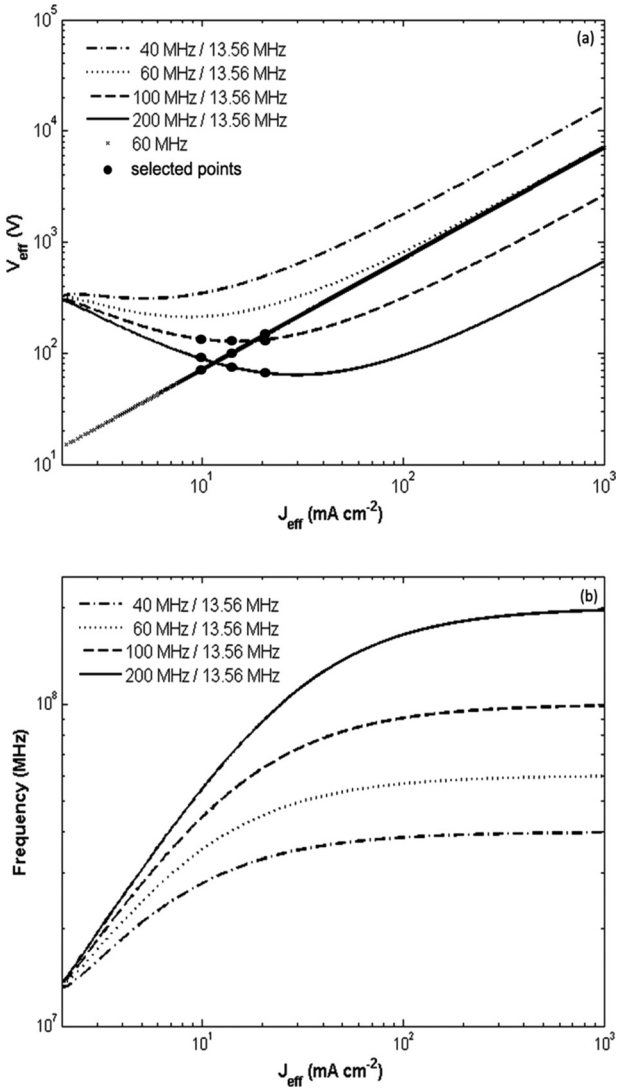

FIG. 1. Effective voltages (a) and effective frequency (b) transitions as a function of effective current in dual rf discharges when the high-frequency ($40 \sim 200$ MHz) current is varied while the low-frequency (13.56 MHz) current ($J_l = 2$ mA cm^{-2}) is fixed.

As a result, the effective voltage decreases with the effective current and it leads to an increase of the ion flux and a decrease of the ion mean energy to the substrate. It is because of this increase in ion flux and decrease in ion energy that the negative resistance regime can be called the preferred regime for solar cell manufacturing. When the value of the larger frequency is very high or when the difference between the two frequencies is large, the transition of the effective frequency is more significant and hence the regime of the negative resistance widens. Comparisons of the plasma characteristics between DF (13.56 MHz/100 MHz and 13.56 MHz/200 MHz) CCP discharges and SF (60 MHz) CCP discharges with the same applied effective current are carried out in this preferred regime.

III. RESULTS AND DISCUSSIONS

To investigate validity of the effective frequency concept, comparisons of plasma characteristics between DF-CCP discharges and its equivalent effective SF-CCP discharges have been carried out. For this purpose, a one-dimensional electrostatic PIC simulation method with an MCC has been used. PIC simulation method with MCC model is a self-consistent method and is capable of taking kinetic affects into account.[10] Simulations have been performed for argon gas discharges with two parallel-plate electrodes separated by the gap distance of 1 cm. Operating gas pressure is taken to be 1 Torr. One or two rf current sources with different frequencies can be applied to the powered electrode at position $x = 0$ cm, while the electrode at position $x = 1$ cm is grounded. The secondary-electron emission coefficient for argon ions is set to be 0.2, while electrons are assumed to be absorbed perfectly at the electrodes. In order to obtain meaningful results in the steady state, all the simulations have been run for several thousand rf cycles. On the basis of analytical calculation of the effective voltage as a function of effective current [Fig. 1(a)], two arbitrary points have been chosen for DF-CCP discharges and these are converted into effective SF-CCP discharges using Eq. (3) or its graphical representation, Figure 1(b). For example, when the low-frequency (13.56 MHz) current is 2 mA cm^{-2} and the high-frequency (100 MHz) current is 19.9 mA cm^{-2}, the effective frequency will be 63 MHz

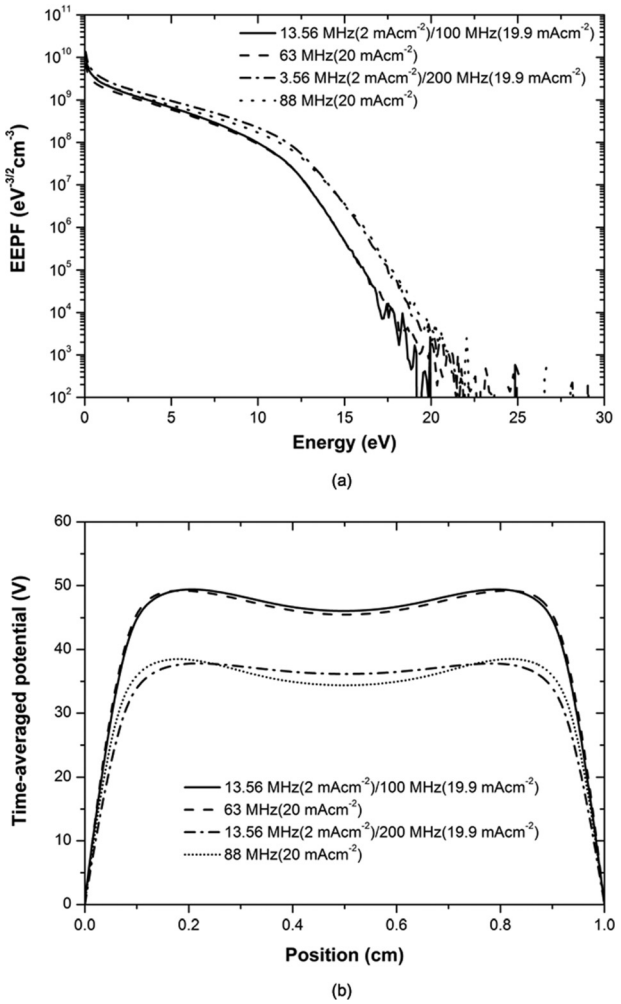

FIG. 2. Electron energy probability functions at the discharge center (a) and time-averaged plasma potential for DF-CCP cases (b) (solid line: 13.56 MHz/100 MHz; dashed-dotted line: 13.56 MHz/200 MHz) and their equivalent effective SF-CCP cases (dashed line: 63 MHz; dotted line: 88 MHz).

with the effective current value of 20 mAcm^{-2}. When the low-frequency (13.56 MHz) current is 2 mA cm^{-2} and the high-frequency (200 MHz) current is 19.9 mA cm^{-2}, the effective frequency will be 88 MHz. PIC/MCC simulation results under theses operating conditions are shown in Figures 2 and 3. Figure 2 shows the electron energy probability functions (EEPF) at the discharge center and time-averaged plasma potential for DF-CCP discharges (13.56 MHz/100 MHz and 13.56 MHz/200 MHz) and for the effective SF-CCP discharges (63 MHz and 88 MHz). As shown in Figure 2, the time-averaged plasma potential and EEPF of DF CCP discharges are in agreement (both qualitatively and quantitatively) with the results of effective SF-CCP discharge. However, as shown in Figure 3, the profiles of ion energy distribution functions (IEDF) of the DF-CCP discharges are different from those of the effective SF-CCP discharges. Figure 3 shows that the IEDFs of the effective SF-CCP discharges have fine structure. These IEDFs on the driven electrode are affected by the ratio of the ion transit time ($\tau_{ion} = 3\bar{s}(M/2e\bar{V}_s)^{1/2}$) to the rf period ($\tau_{rf} = 2\pi/\omega_{eff}$).[6,19] This ratio can be expressed as a function of effective frequency, sheath length, and average potential difference between driven electrode and the bulk plasma and is given by

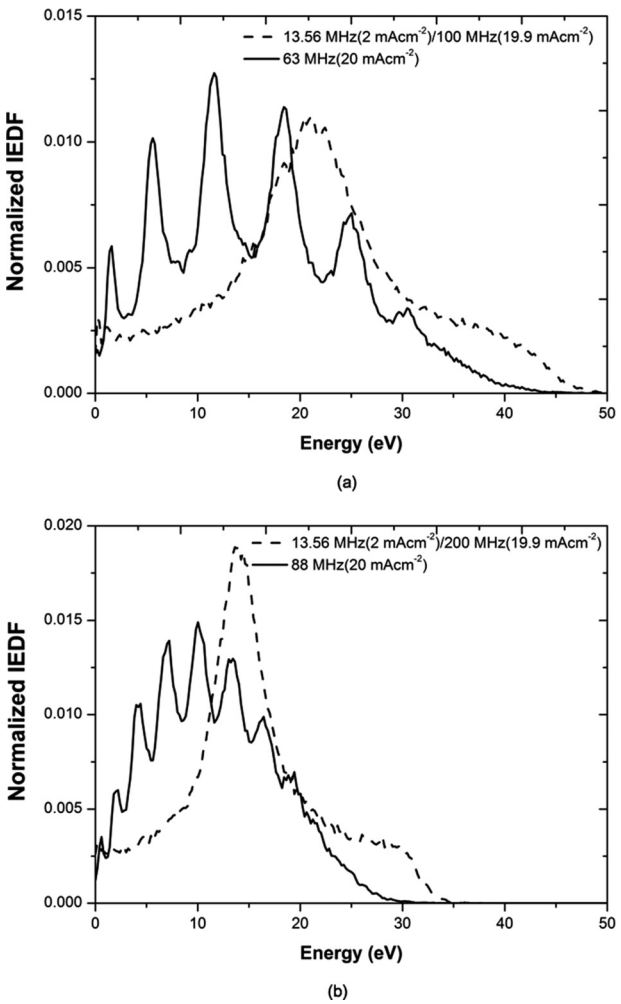

FIG. 3. Normalized IEDFs on the driven electrode for the effective frequency of (a) 63 MHz and (b) 88 MHz with the effective current of 20 mA cm^{-2}.

$$N = \frac{\tau_{ion}}{\tau_{rf}} = \frac{3\bar{s}(M/2e\bar{V}_s)^{1/2}}{2\pi/\omega_{eff}}. \quad (7)$$

Here M is the argon ion mass and e is the electron charge (1.602×10^{-19} C). Time-averaged sheath voltage and time-averaged sheath length needed for the calculation of ion transit time are obtained from PIC/MCC simulations. In the case of 88 MHz ($J_{eff} = 20$ mAcm^{-2}), the ion transit time and the rf period are 0.0824 μs and 0.0114 μs, respectively. The ratio of the ion transit time to the rf period is 7.25. In the case of 63 MHz ($J_{eff} = 20$ mAcm^{-2}), the ion transit time and the rf period are 0.0884 μs and 0.0159 μs, respectively, and the ratio of the ion transit time to the rf period is 5.57. It means that the ion transit time through the sheath (τ_{ion}) is greater than the rf period (τ_{rf}). Moreover, there are few charge-exchange collisions within the sheath length, which results in fine structure like IEDF similar to low pressure discharges.[6] In other words, these peaks correspond to those slow ions which are created in the sheath as results of charge-exchange collisions or ionization in the sheath. These slow ions are accelerated by the time and space varying sheath potential. The number of peaks can be roughly estimated as the ratio (Eq. (7)) of the ion transit time to the rf period.[21] For $f_{rf} = 63$ MHz ($J_{eff} = 20$ mAcm^{-2}), the number of peaks should be 5 or 6. For $f_{rf} = 88$ MHz ($J_{eff} = 200$ mAcm^{-2}), the number of peaks should be 7 or 8. These numbers are in agreement with the number of peaks obtained in the simulation results (Figure 3). On the other hand, in case of DF-CCP discharge, the fine structure observed in the SF-CCP discharge is destroyed and the single peak structure is observed. This structure is due to the presence of low frequency. It is assumed that low frequency current source controls the acceleration of the ions and determines the ion mean energy when there is substantial frequency difference between high and low frequency (i.e., $f_{hf} \gg f_{lf}$). Under these conditions the ratios τ_{ion}/τ_{eff} and τ_{ion}/τ_{hf} are much larger than one, however, the ratio τ_{ion}/τ_{lf} is almost one. Because of that the number of peaks obtained in the simulation is smaller than that obtained from Eq. (7). In the regime where $\tau_{ion}/\tau_{eff} \gg 1$ for single and dual rf discharges, ions respond to the time-averaged sheath voltage because ions cross the sheath in a time corresponding to many rf cycles but the ion mean energy is smaller than the time-averaged plasma potential (=sheath potential). The ion mean free path (<40 μm) is smaller than the sheath width (~300 μm) and, therefore, ions lose their energy through collisions with the background neutral gas inside the sheaths. Even though the profiles of IEDFs are different, the plasma characteristics (such as plasma potential, EEPF, density, and ion mean energy) of DF-CCP discharge and its effective SF counterpart are almost same, so DF CCP can be analyzed in a fashion similar to SF driven CCP discharge with effective parameters. The comparison study between these simulation results and the experimental measurements is planned for a future publication.

The effective voltage can be observed as a function of effective current for estimation of the ion mean energy in dual and single rf discharges by using this effective frequency concept [Figure 1(a)]. In view of the low ion

bombardment energy required for the high-quality thin films, direct comparison between DF and SF CCP discharges at the same applied rf current is possible. As shown in Figure 1(a), 9 points in the negative resistance regime are chosen to compare plasma characteristics of DF CCP discharge to those of SF CCP discharge. In DF (13.56 MHz/100 MHz and 13.56 MHz/200 MHz) and SF (60 MHz) CCP discharges, 1-D PIC/MCC simulations are carried out for various values of the applied rf effective currents (10, 15, and 20 mA cm^{-2}). Figure 4 shows the simulation results of time-averaged plasma potential for the effective current of 10 mA cm^{-2}, 15 mA cm^{-2}, and 20 mA cm^{-2} in single and dual frequency discharges. As shown in Figure 4, when the effective current is 10 mA cm^{-2}, the mean energy in case of DF CCP (13.56 MHz/100 MHz and 13.56 MHz/200 MHz) discharges is larger than that of SF CCP (60 MHz) discharge. On the other hand, when the effective current is 20 mA cm^{-2}, the mean energy of the DF CCP discharges is smaller than that of the SF CCP discharge. When the effective current is 15 mA cm^{-2}, the ion mean energy of SF CCP discharge is larger than that of DF CCP (13.56 MHz/200 MHz) discharge, but smaller than that of DF CCP (13.56 MHz/100 MHz) discharge. As shown in Figure 4, the PIC/MCC simulation results for the mean energy are in qualitative agreement with the analytical results [Fig. 1(a)] in a collisionless rf sheath model through the effective frequency. Using our analytic global model, we found the negative resistance phenomenon as shown in Figure 1(a) and it is also found in 1D PIC/MCC simulation as our expectation as shown in Figure 4. Figure 5 shows the ion peak density at the discharge center as a function of the effective current. Because the plasma density is proportional to the applied effective rf current ($n \propto J_{rf}$), the ion peak density increases with the effective current in single and dual frequency discharges. As shown in Figures 4 and 5, at the lower effective current density (or at the lower plasma density), the mean ion energy of SF CCP discharge is lower than that of DF CCP discharge. At the higher effective current density (or at the higher plasma density), however, the mean ion energy of DF CCP discharge is lower than that of SF CCP discharge.

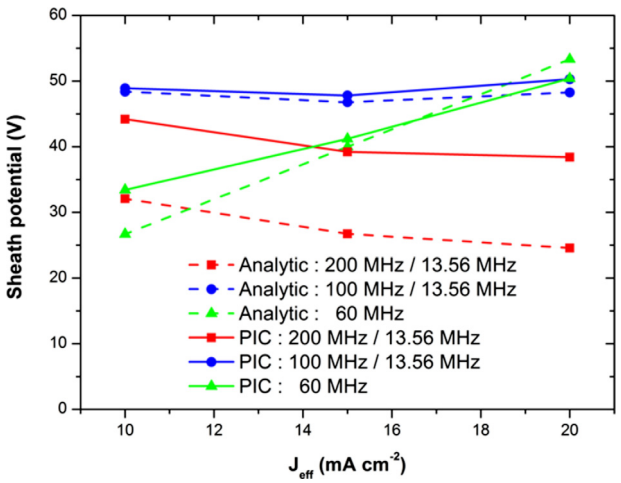

FIG. 4. (Color online) Comparison between simulated(solid line) and analytically calculated(dashed line) sheath potential for the effective current of 10 mA cm^{-2}, 15 mA cm^{-2}, and 20 mA cm^{-2} in single (triangle symbol: 60 MHz) and dual (circle symbol: 13.56 MHz/100 MHz; square symbol: 13.56 MHz/200 MHz) rf discharges.

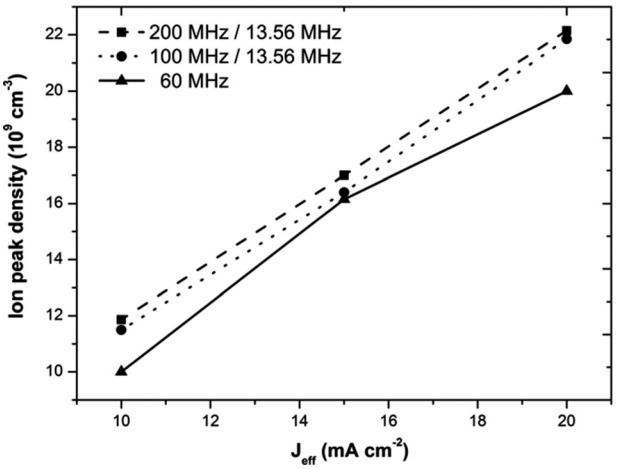

FIG. 5. The ion peak density at the discharge center as a function of the effective current.

IV. CONCLUSION

The validity of the effective frequency concept that a DF CCP discharge can be considered as a SF CCP discharge driven with effective parameters has been investigated to enhance our understanding of the DF CCP discharges. It is shown that plasma characteristics such as plasma potential, EEPF, density, and ion mean energy of the DF CCP discharge and its effective SF counterpart are almost same even though the profiles of IEDFs are different. So this concept can be applied to understand physics of DF CCP discharges and to find the optimum regime for use of these discharges for PECVD. The analytical calculations of the plasma characteristics in dual frequency discharges through the effective frequency concept performed in this study are in qualitative agreement with the simulation results calculated by using 1D PIC/MCC model. Using this concept, one can obtain the effective voltage related to the ion mean energy as a function of applied effective current in dual rf discharges. From these results, one can observe the negative resistance regime, which is a unique physical phenomenon that happens in DF CCP discharges. In this regime, the effective voltage decreases with the effective current and it leads to an increase of the ion flux and a decrease of the ion mean energy and can be called the preferred regime for solar cell manufacturing. In this preferred regime, comparison of DF and SF CCP discharges with the same effective current density is carried out. When the effective current density is low (or the plasma density is low), the ion mean energy of SF CCP discharge is lower than that of the DF CCP discharge. When the effective current density is high (or the plasma density is high), however, the ion mean energy of DF CCP discharge is lower than that of SF CCP discharge. These conditions can be used to increase the plasma density and hence deposition rate without damaging the substrate surface as the ion mean energy is low. Using DF CCP discharge under these circumstances is better than using SF CCP discharge for solar cell manufacturing processes.

ACKNOWLEDGMENTS

This work was supported by SEMES and the National Research Foundation of Korea Grants (NRF-2010-355-D00089 and 2011-0015395) and the Brain Korea 21 program funded by the Korean Government (Ministry of Education, Science, and Technology).

[1]T. Makabe and K. Maeshige, Appl. Surf. Sci. **192**, 176 (2002).
[2]T. Kitajima, Y. Takeo, Z. Lj. Petrovic, and T. Makabe, Appl. Phys. Lett. **77**, 489 (2000).
[3]H. H. Goto, H.-D. Lowe, and T. Ohmi, IEEE Trans. Semicond. Manuf. **6**, 58 (1993).
[4]S. Rauf and M. J. Kushner, IEEE Trans. Plasma Sci. **27**, 1329 (1999).
[5]H. C. Kim, J. K. Lee, and J. W. Shon, Phys. Plasmas **10**, 4545 (2003).
[6]J. K. Lee, O. V. Manuilenko, N. Yu. Babaeva, H. C. Kim, and J. W. Shon, Plasma Sources Sci. Technol. **14**, 89 (2005).
[7]H. C. Kim and J. K. Lee, Phys. Rev. Lett. **93**, 085003 (2004).
[8]P. C. Boyle, A. R. Ellingboe, and M. M. Turner, J. Phys. D **37**, 697 (2004).
[9]Z.-H. Bi, Y.-X. Liu, W. Jiang, X. Xu, and Y.-N. Wang, Curr. Appl. Phys. **11**, S2 (2011).
[10]H. C. Kim, F. Iza, S. S. Yang, M. Radmilovic-Radjenovic, and J. K. Lee, J. Phys. D: Appl. Phys. **38**, R283 (2005).
[11]M. A. Lieberman and A. J. Lichtenberg, *Principles of Plasma Discharges and Materials Processing* (Wiley, New York, 2005).
[12]T. Makabe and Z. Petrovic, *Plasma Electronics: Applications in Microelectronic Device Fabrication* (Taylor and Francis, New York and London, 2006).
[13]B. Kalache, A. I. Kosarev, R. Vanderhaghen, and P. Roca i Cabarrocas, J. Non-Cryst. Solids **299**, 63 (2001).
[14]U. Kroll, A. Shah, H. Keppner, J. Meier, P. Torres, and D. Fischer, Sol. Energy Mater. Sol. Cells **48**, 343 (1997).
[15]T. Roschek, T. Repmann, J. Muller, B. Rech, and H. Wagner, J. Vac. Sci. Technol. A **20**, 492 (2002).
[16]Y. Mai, S. Klein, R. Carius, J. Wolff, A. Lambertz, F. Finger, and X. Geng, J. Appl. Phys. **97**, 114913 (2005).
[17]S. Q. Xiao and S. Xu, J. Phys. D: Appl. Phys. **44**, 174033 (2011).
[18]H. C. Kim and J. K. Lee, J. Vac. Sci. Technol. A **23**, 651 (2005).
[19]S. H. Lee, P. K. Tiwari, and J. K. Lee, Plasma Sources Sci. Technol. **18**, 025024 (2009).
[20]T. H. Chung, Phys. Plasmas **12**, 104503 (2005).
[21]C. Wild and P. Koidl, J. Appl. Phys. **69**, 2909 (1991).